

AD-A106 479

AEROSPACE CORP EL SEGUNDO CA SPACE SCIENCES LAB
THE ROLE OF HISS IN MAGNETOSPHERIC CHORUS EMISSIONS.(U)
SEP 81 H C KOONS

F/G 4/1

UNCLASSIFIED

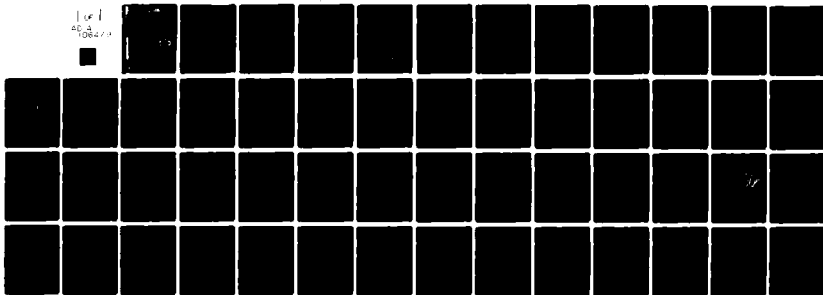
TR-0081(6960-06)-10

SD-TR-81-77

F04701-80-C-0081

NL

1 of 1
AD-A106 479



END

DATE

FILED

11-81

DTIC

(12)

LEVEL II

AD A106479

The Role of Hiss in Magnetospheric Chorus Emissions

H. C. KOONS
Space Sciences Laboratory
Laboratory Operations
The Aerospace Corporation
El Segundo, Calif. 90245

28 September 1981

DTIC
ELECTE
NOV 2 1981
B

APPROVED FOR PUBLIC RELEASE;
DISTRIBUTION UNLIMITED

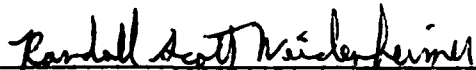
Prepared for
SPACE DIVISION
AIR FORCE SYSTEMS COMMAND
Los Angeles Air Force Station
P.O. Box 92960, Worldway Postal Center
Los Angeles, Calif. 90009


81103003 9

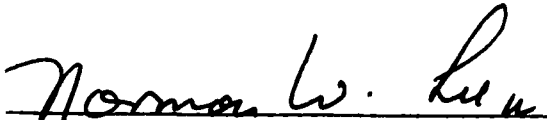
This report was submitted by The Aerospace Corporation, El Segundo, CA, 90245, under Contract No. F04701-80-C-0081 with the Space Division, Deputy for Technology, P.O. Box 92960, Worldway Postal Center, Los Angeles, CA 90009. It was reviewed and approved for The Aerospace Corporation by G.A. Paulikas, Director, Space Sciences Laboratory. Lt R. S. Weidenheimer, SD/YLVS, was the project officer for Mission-Oriented Investigation and Experimentation (MOIE) Programs.

This report has been reviewed by the Public Affairs Office (PAS) and is releasable to the National Technical Information Service (NTIS). At NTIS, it will be available to the general public, including foreign nations.

This technical report has been reviewed and is approved for publication. Publication of this report does not constitute Air Force approval of the report's findings or conclusions. It is published only for the exchange and stimulation of ideas.


Randall S. Weidenheimer, 2nd Lt, USAF
Project Officer


Florian P. Meinhardt, Lt Col, USAF
Director of Advanced Space Development


Norman W. Lee, Jr., Colonel, USAF
Deputy for Technology

UNCLASSIFIED

SECURITY CLASSIFICATION OF THIS PAGE (When Data Entered)

REPORT DOCUMENTATION PAGE		READ INSTRUCTIONS BEFORE COMPLETING FORM
1. REPORT NUMBER SD-TR-81-77	2. GOVT ACCESSION NO. AD-A106479	3. RECIPIENT'S CATALOG NUMBER
4. TITLE (and Subtitle) THE ROLE OF HISS IN MAGNETOSPHERIC CHORUS EMISSIONS.		5. TYPE OF REPORT & PERIOD COVERED
7. AUTHOR(s) Harry C./Koons		6. PERFORMING ORG. REPORT NUMBER TR-0081(6960-06)-10
9. PERFORMING ORGANIZATION NAME AND ADDRESS The Aerospace Corporation El Segundo, Calif. 90245		8. CONTRACT OR GRANT NUMBER(s) F04701-80-C-0081 NSF-A1139 17969
11. CONTROLLING OFFICE NAME AND ADDRESS Space Division Air Force Systems Command Los Angeles, Calif. 90009		10. PROGRAM ELEMENT, PROJECT, TASK AREA & WORK UNIT NUMBERS 125
14. MONITORING AGENCY NAME & ADDRESS (if different from Controlling Office)		12. REPORT DATE 28 September 1981
		13. NUMBER OF PAGES 54
		15. SECURITY CLASS. (of this report) Unclassified
		15a. DECLASSIFICATION/DOWNGRADING SCHEDULE
16. DISTRIBUTION STATEMENT (of this Report) Approved for public release; distribution unlimited		
17. DISTRIBUTION STATEMENT (of the abstract entered in Block 20, if different from Report)		
18. SUPPLEMENTARY NOTES		
19. KEY WORDS (Continue on reverse side if necessary and identify by block number) Very Low Frequency Chorus Emissions Hiss Emissions Cyclotron Resonance		
20. ABSTRACT (Continue on reverse side if necessary and identify by block number) Many researchers have reported that narrowband hiss emissions are simultaneously present with ELF chorus emissions outside of the plasmasphere. In data from the SCATHA satellite chorus emissions are often observed to start at frequencies that are within a hiss band. Hiss band spectra averaged for 6.4 s with a resolution of 5 Hz are very smooth. Relative maxima are typically less than 2 db above adjacent minima. Spectra obtained on a 200 ms sample show large variations in amplitude between adjacent bins with relative maxima 10 to 15 db above adjacent		

DD FORM 1473
(FACSIMILE)

UNCLASSIFIED

SECURITY CLASSIFICATION OF THIS PAGE (When Data Entered)

UNCLASSIFIED

SECURITY CLASSIFICATION OF THIS PAGE(When Data Entered)

19. KEY WORDS (Continued)

20. ABSTRACT (Continued)

minima. Electrons in a narrow range of energies and pitch angles can be organized in phase by the doppler-shifted cyclotron resonance with the larger amplitude spectral components in the hiss band. The bandwidth of the cyclotron resonance is found to be sufficiently narrow so that the electrons are not dephased by waves in adjacent portions of the highly structured spectrum. The amplitude of the hiss is sufficient to significantly phase bunch the electrons in the calculated interaction time. The chorus emission is then generated as the phase bunched electrons moved adiabatically along the geomagnetic field line. No evidence for monochromatic input waves such as power line harmonic radiation are found in the SCATHA data within the hiss bands from which chorus is observed to be triggered. This mechanism can also account for the chorus emissions detected at frequencies above a hiss band in the Jovian magnetosphere.

UNCLASSIFIED

SECURITY CLASSIFICATION OF THIS PAGE(When Data Entered)

PREFACE

The author is indebted to L. Christopher, B. Edgar, L. Friesen, W. B. Harbridge, C. Hetlinger and R. Maulfair for their contributions to this project. This work was supported in part by the National Science Foundation under Grant ATM80-19060 and in part by the U. S. Air Force under Contract F04701-80-C-0081.

Accession For	
NTIS GRA&I	<input checked="checked" type="checkbox"/>
DTIC TAB	<input type="checkbox"/>
Unannounced	<input type="checkbox"/>
Justification	
By	
Distribution/	
Availability Codes	
Dist	Avail and/or Special
A	

CONTENTS

PREFACE.....	1
I. INTRODUCTION.....	9
II. DESCRIPTION OF EXPERIMENT.....	15
III. DATA.....	19
IV. PARAMETRIC ANALYSIS.....	29
V. NUMERICAL EXAMPLE.....	39
VI. POWER LINE RADIATION.....	49
VII. CONCLUSIONS.....	53
REFERENCES.....	55

FIGURES

1.	Chorus emissions emerging from hiss bands.....	12
2.	Chorus emissions emerging from hiss band on April 6, 1979 at L = 6.06 at 11:48 LT.....	13
3.	Frequency response of the broadband magnetic field channel of the SCATHA VLF receiver.....	16
4.	Measured wave amplitudes as a function of the angle between the antenna axis and the geomagnetic field direction.....	20
5.	Wave amplitudes as a function of the angle between the antenna axis and the geomagnetic field direction.....	21
6.	Wave amplitudes as a function of the angle between the antenna axis and the geomagnetic field direction.....	22
7.	Hiss band spectra.....	25
8.	Hiss band spectra.....	26
9.	Hiss band spectra.....	27
10.	The intrinsic bandwidth of the doppler-shifted cyclotron resonance of energetic electrons with whistler-mode waves at the magnetic equator at L = 6 as a function of the electron density.....	33
11.	The energy of electrons with a pitch angle of 30 deg resonant with whistler-mode waves at the magnetic equator at L = 6 as a function of the electron density.....	34
12.	The wave-particle interaction time (solid curves) and the electron phase-bunching time (dashed curve) at the magnetic equator at L = 6 as a function of the electron density.....	35
13.	Individual hiss band spectrum obtained from a 200-ms data sample from the magnetic antenna on July 19, 1979.....	36
14.	Parametric fit to a chorus element in Fig. 15.....	40

FIGURES (Continued)

15. (left) Chrous elements computed using the parameters in Table 1 and a ray tracing program to obtain the time delays as a function of frequency for nonducted propagation to a detector located at the specified L-shell and magnetic latitudes, λ 41
16. Typical nonducted chorus ray paths from the point of emission to the SCATHA satellite located on $L = 6.06$ at a magnetic latitude of 3.36 deg..... 45
17. Measured frequency differences between dominant maxima in the hiss band spectra and the nearest power line harmonic..... 51

TABLES

1.	Parameters for the Chorus Events Studied.....	24
2.	Chorus Element Model Parameters.....	44

I. INTRODUCTION

Chorus emissions are extremely-low-frequency (ELF) electromagnetic waves that are commonly observed outside of the plasmasphere [Burtis and Helliwell, 1976; Tsurutani and Smith, 1974; 1977]. They are characterized as discrete emissions usually rising rapidly in frequency with time. Dowden [1962] showed that doppler-shifted cyclotron radiation from electrons moving adiabatically along a geomagnetic field line gives frequency-time spectra similar to those of very-low-frequency emissions observed on the ground. He later showed [Dowden, 1971] that hook emissions are generated symmetrically in time and space about the equatorial plane. He carefully notes that symmetrical generation does not mean that the emission is generated at the equatorial plane.

Burton and Holzer [1974] report wave-normal measurements of chorus emissions. Their measurements were limited to frequencies below 1000 Hz. They assign only one wave-normal value to each emission. This was obtained by integrating the wave normal over one element, giving a mean value. Cornilleau-Wehrlin et al. [1976] extended this type of analysis by determining the wave normal angle as a function of time during the course of an element, without any averaging. They found that the wave normal direction turns meaningfully with respect to the static magnetic field during some elements. In one of the three examples of rising elements that they analyzed the wave normal angle turns from 60° to 20° systematically in about 100 ms. Several of the details of the wave generation as described by Burton and Holzer [1974] are inconsistent with the SCATHA data described below. These inconsistencies include 1) the assumption that the waves are generated in a localized region near the equator, 2) the conclusion that the generation cone is limited to a half-angle of about 20° with respect to the geomagnetic field, and 3) the

conclusion that there is rapid attenuation of unducted chorus with wave-normal angles greater than 25° . We find that all of these conditions must be relaxed to obtain the full spectral shape from the doppler-shifted cyclotron radiation mechanism.

Recent attention has been directed toward the mechanism for phase bunching the electrons such that an embryo emission [Dowden et al., 1978] can be generated. Conflicting evidence has been presented. Lurette et al. [1977] show that VLF chorus activity observed by the OGO-3 satellite shows significant longitudinal variations which they interpret as evidence of excitation by power line radiation. Lurette et al. [1979] present evidence that radiated power line harmonic radiation (PLR) leaks into high-altitude regions of the magnetosphere with sufficient intensity to control the starting frequencies of chorus emissions. They conclude that man-made VLF noise plays an important role in the generation of chorus. However Tsurutani et al. [1979] analyzing OGO-5 data found no statistically significant correlation between longitude and chorus occurrence. They conclude that they were unable to find any evidence for a significant effect of power line radiation on the stimulation of chorus. They suggest that the longitudinal variations found by Lurette et al. [1977] are invalid and were an effect of data oversampling in the method of analysis.

Overlooked in this debate is a growing body of evidence that magnetospheric hiss is almost always present when chorus is observed by satellites near the equator. Burtis and Helliwell [1976] note that chorus was often accompanied by a background of hiss having a variable amount of structure. Burtis [1969] called this unstructured noise 'banded hiss' because of its tendency to accompany band limited chorus. Cornilleau - Wehrlin et al. [1978] present the statistical occurrence of hiss and chorus beyond six earth radii

when $K_p \leq 2^+$. They note that the simultaneous occurrence of hiss and chorus is an almost permanent situation. They recognize that the presence of the hiss has important implications with respect to the theories of chorus generation and suggest that some kind of VLF turbulence must be present before the strong chorus emission process can start.

We thus find two diametrically opposite possibilities. First that of Lurette et al. [1977, 1979] that a monochromatic input wave from powerline harmonic radiation plays an important role in the generation of chorus. Second that of Cornilleau Wehrlin et al. [1978] that VLF turbulence (hiss) plays an important role in the generation of chorus.

We finally note the simultaneous occurrence of hiss and chorus observed by Voyager-1 in the Jovian Magnetosphere [Coroniti et al., 1980]. This certainly proves that powerline radiation in a magnetosphere is not a necessary condition for chorus emissions and adds further credence to a possible role for hiss in chorus generation.

We have produced spectrograms from several hundred hours of broadband VLF data from the U.S. Air Force P78-2 (SCATHA) satellite. We find that chorus is a common emission and in agreement with Burtis and Helliwell [1976] and Cornilleau-Wehrlin et al. [1978] we find that chorus and hiss generally occur simultaneously.

We find one additional characteristic that gives a clue to the emission mechanism. Frequently the chorus emissions are observed to start at frequencies that are within a hiss band. Examples of such discrete emissions emerging from hiss bands are shown in Figs 1 and 2.

In this paper we show that chorus emission is a natural stochastic process that can occur within highly structured hiss bands in the outer magneto-

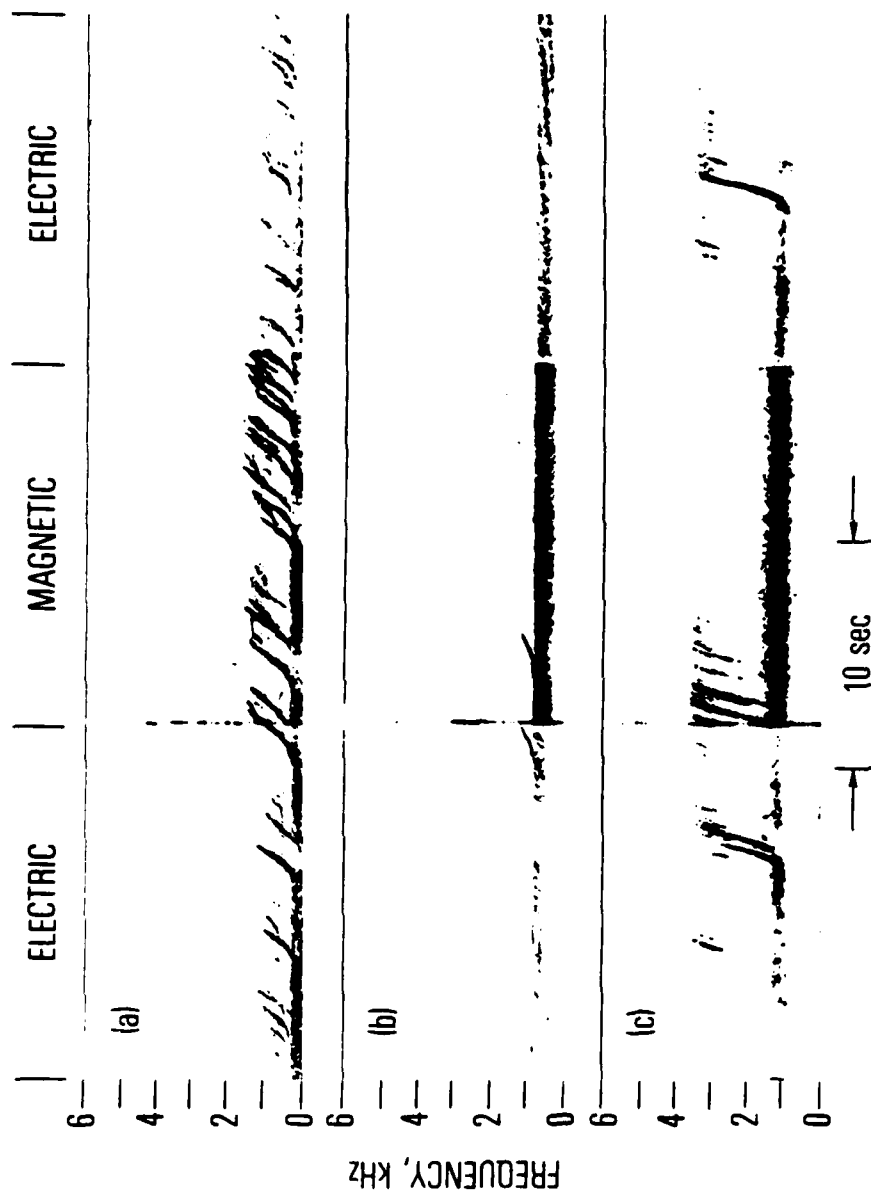


Figure 1. Chorus emissions emerging from hiss bands. (a) August 30, 1979 at L=6.92 at 15:42 LT, (b) July 9, 1979 at L=6.8 at 18:36 LT, (c) July 19, 1979 at L=6.01 at 15:24 LT.

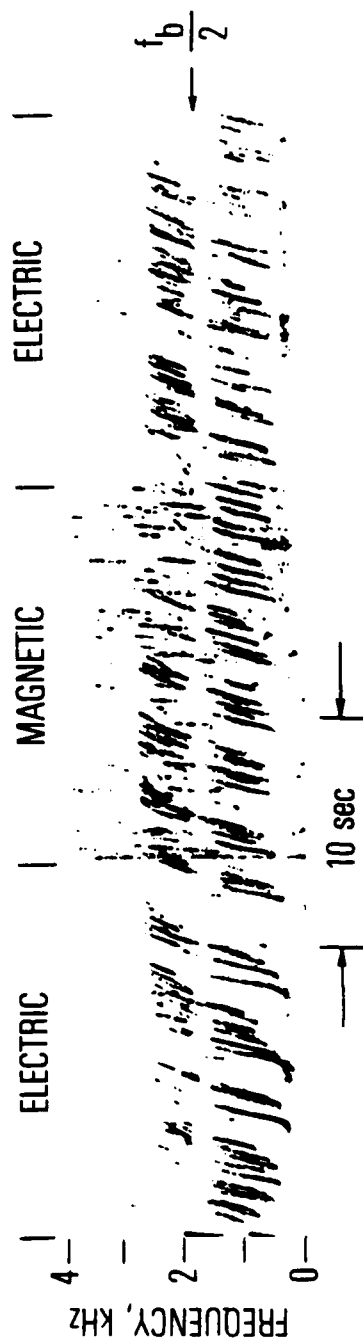


Figure 2. Chorus emissions emerging from hiss band on April 6, 1979 at
L=6.06 at 11:48 LT.

sphere.

To do this we show that hiss is polarized with the field components nearly perpendicular to the geomagnetic field line, that there are large local maxima in the spectrum on the time scale of the wave-particle interaction time in the band, and that electrons in a narrow range of energies and pitch angles can be phase bunched by these waves. Doppler-shifted cyclotron radiation from these phase-bunched electrons then produce the chorus emission. We finally show that there is no evidence that monochromatic input waves such as power-line harmonic radiation are present in the hiss band to phase bunch the electrons.

II. DESCRIPTION OF EXPERIMENT

The P78-2 (SCATHA) spacecraft was launched from the Eastern Test Range at 21 h 42 m UT on 30 January 1979. The final orbit was equatorial with a 23 h 35 m period, a 7.9 deg inclination, a 7.78 earth radii apogee and a 5.32 earth radii perigee. The spacecraft was spin stabilized with a spin rate of one rpm. The spin vector is in the orbital plane and is maintained perpendicular (± 5 deg) to the sun-satellite line.

The VLF Receiver measures emissions in the frequency range from 10's of Hz to 300 kHz. The experiment employs two antennas to distinguish electrostatic and electromagnetic emissions. An air-core loop antenna detects the magnetic component of the waves and a 100-m tip-to-tip dipole, provided by the Goddard Space Flight Center for the DC Electric Field Experiment, detects the electric component.

The sensitivity of the electric field receiver is 5×10^{-7} V/m $\sqrt{\text{Hz}}$ at 1.3 kHz and 10^{-7} V/m $\sqrt{\text{Hz}}$ at 10.5 kHz. The air-core loop is electrostatically shielded and has an effective area of 575 m² at 1.3 kHz. It is constructed of 1530 turns of 36 AWG copper wire on a form 50 cm in diameter. The antenna is boom mounted 2 m from the body of the spacecraft. The sensitivity of the receiver is 3×10^{-6} $\gamma/\sqrt{\text{Hz}}$ at 1.3 kHz. The frequency response of the magnetic section is shown in Fig. 3. The dynamic range is 60 db.

The receiver can process signals from only one antenna at a time. The antenna is normally switched every 16 s.

The receiver has a narrowband and a broadband mode. The primary on-orbit operational mode is the narrowband filter mode providing continuous tape recorded data. There are eight narrowband channels at 0.4, 1.3, 2.3, 3.0,

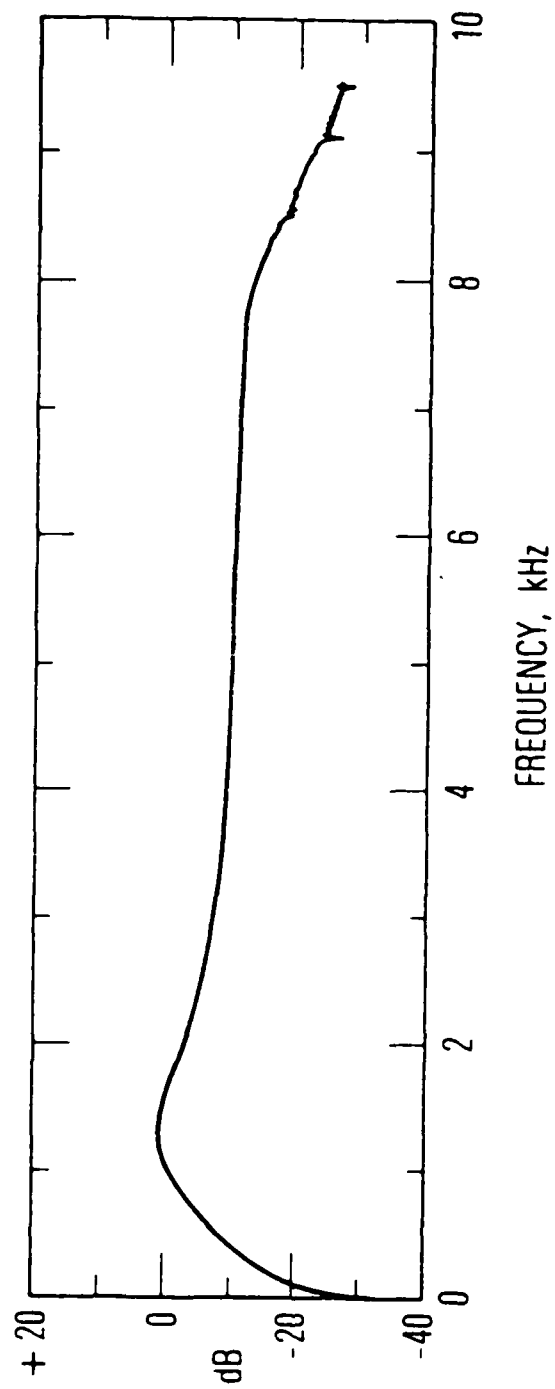


Figure 3. Frequency response of the broadband magnetic field channel of the SCATHA VLF receiver.

10.5, 30, 100 and 300 kHz. Each channel is sampled two times per second. The bandwidth of each channel is $\pm 7.5\%$ of its center frequency. There are two broadband modes, 0 to 3 kHz and 0 to 5 kHz. The broadband data can only be collected in real time. One to two hours of broadband data have been collected each day.

III. DATA

The examples of chorus and hiss shown in Figs. 1a, 1c and 2, were chosen for analysis because the hiss bands fall within the frequency range of either the 400 Hz or the 1.3 kHz narrowband channels of the receiver. The gaps in the hiss bands during a strong emission are caused by a reduction in sensitivity due to the Automatic Gain Control (AGC) circuitry in the broadband section of the receiver. The AGC does not affect the narrowband channel data. The narrowband data can thus be used to accurately measure the wave intensities of the hiss and the wave-normal distributions in the plane of the antenna rotation.

The electric and magnetic field intensities at 400 Hz and 1.3 kHz for a 10 min interval around the time of the data shown in Fig. 2 are plotted in Fig. 4 as a function of the angles of the appropriate antenna axis with respect to the geomagnetic field. In Fig. 5 the data have been logarithmically averaged in two degree bins. The 400 Hz data represents the hiss and the 1.3 kHz represents the chorus. In Fig. 6 averaged data are plotted for a 40 min time period about the time of the example shown in Fig. 1c. Here both the 400 Hz and 1.3 kHz data are from portions of the spectrum occupied by the hiss band.

The hiss intensity is relatively constant. The wave field components maximize perpendicular to the magnetic field vector, \vec{B}_0 . There are 15 db nulls parallel to the field. This shows that the wave normal vector \vec{k} , is nearly parallel to \vec{B}_0 . The chorus measured at 1.3 kHz has large variations in amplitude which mask any angular dependence.

We have spectrum analyzed the data from twenty acquisitions during which chorus emissions originate in hiss bands. The parameters for these twenty

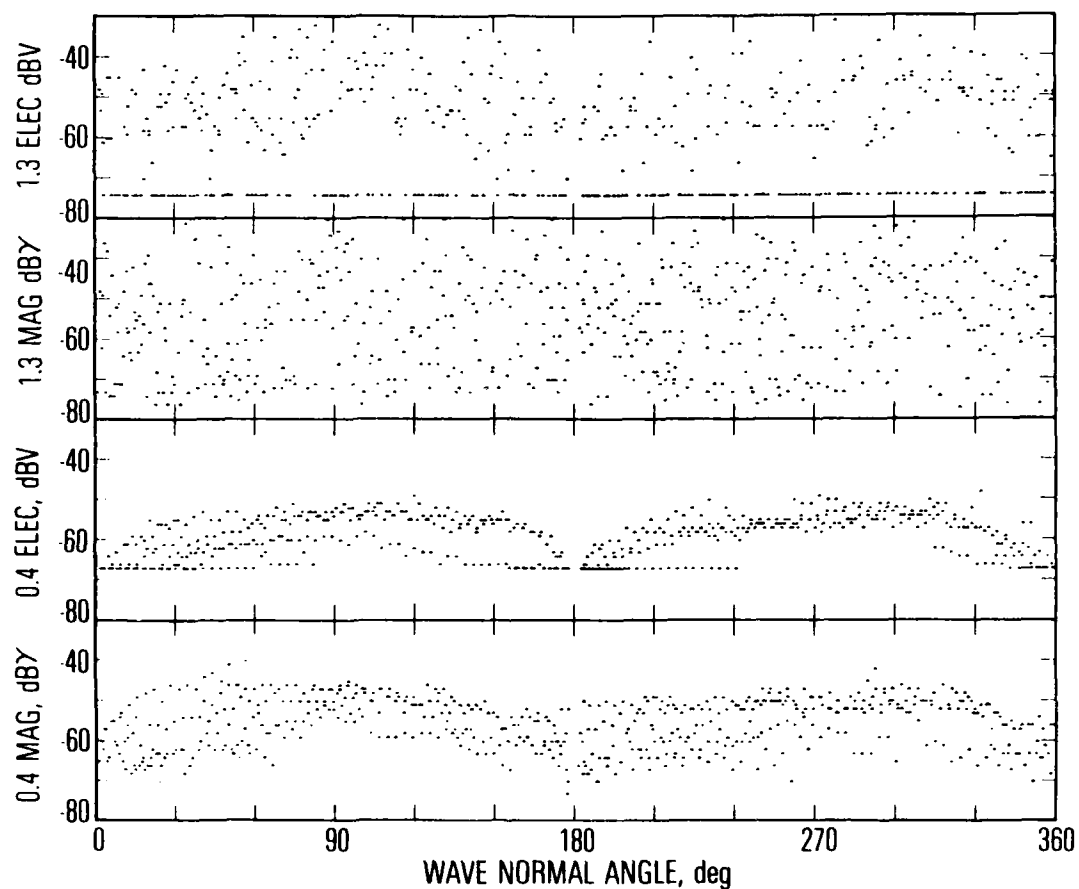


Figure 4. Measured wave amplitudes as a function of the angle between the antenna axis and the geomagnetic field direction. These data were obtained between 04:30 and 04:40 UT on April 6, 1979. This time period contained the emissions shown in Fig. 2.

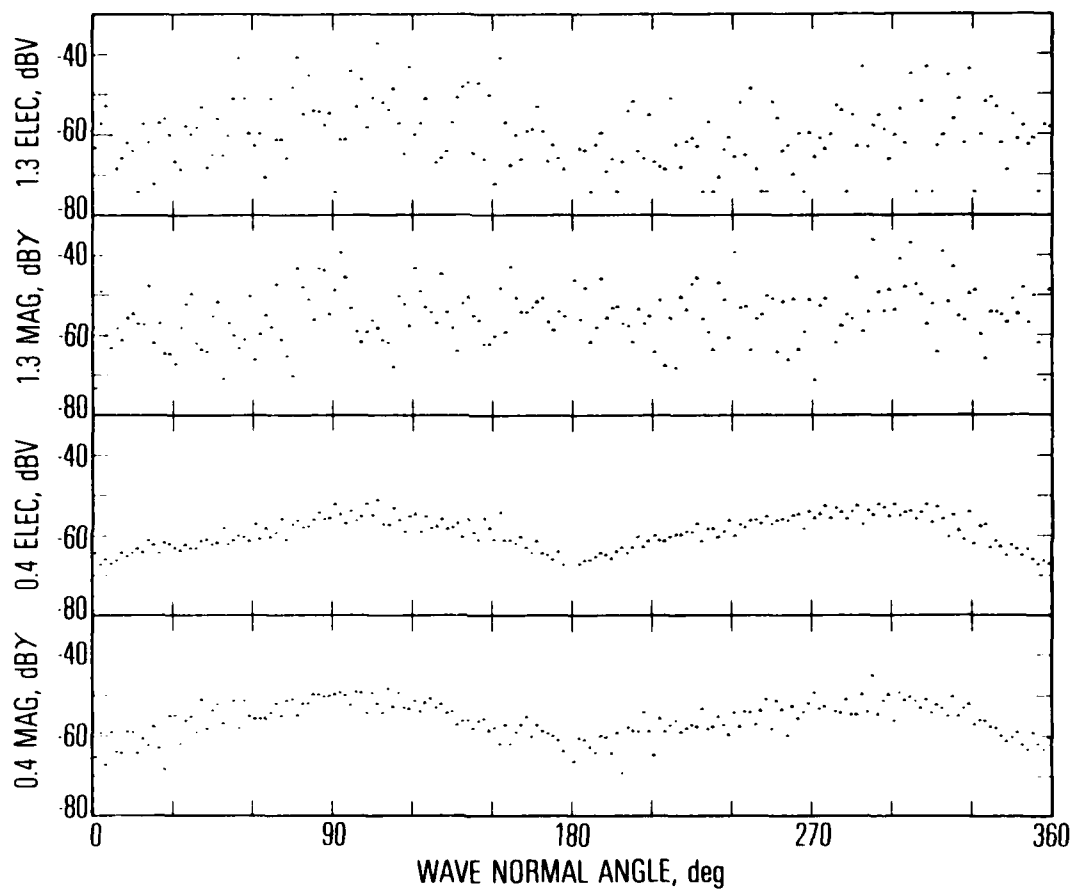


Figure 5. Wave amplitudes as a function of the angle between the antenna axis and the geomagnetic field direction. The data are logarithmic averages in two degree bins of the data shown in Fig. 4.

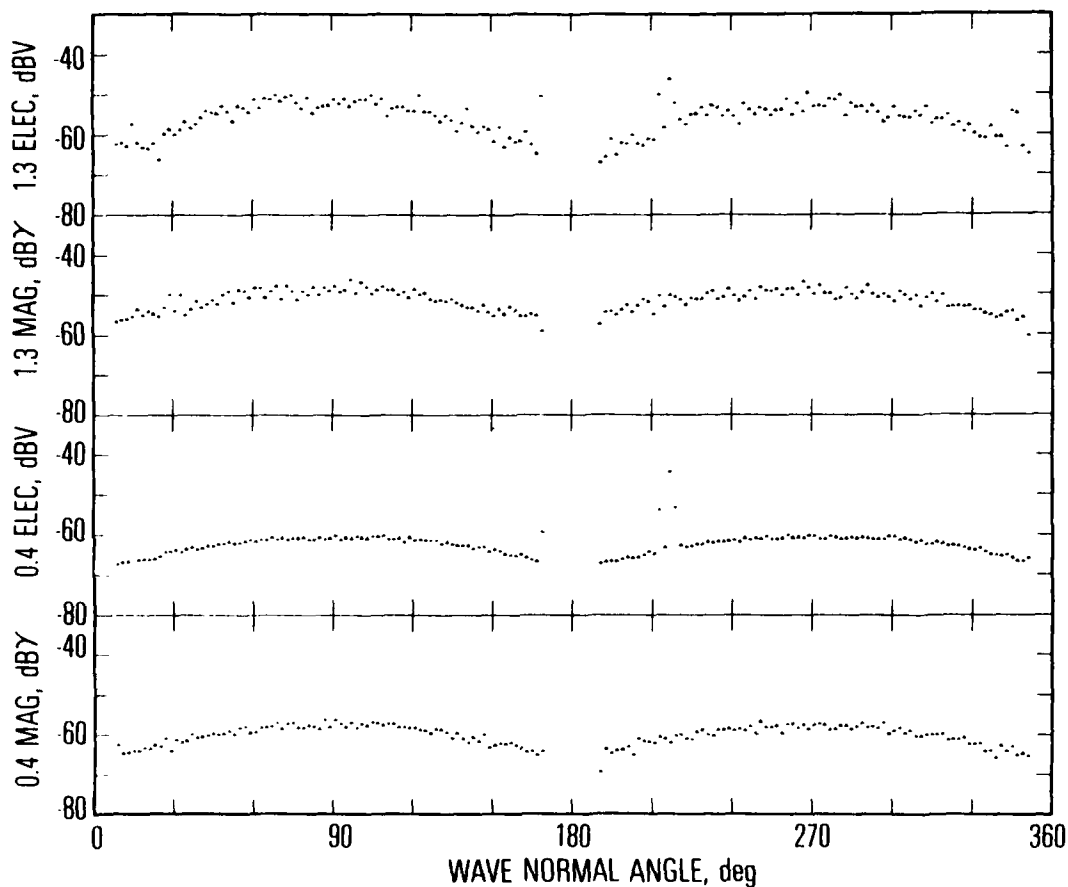


Figure 6. Wave amplitudes as a function of the angle between the antenna axis and the geomagnetic field direction. The data are logarithmic averages in two degree bins. The measurements were obtained between 17:20 and 18:00 UT on July 19, 1979. This time period corresponds with the spectrogram shown in Fig. 1c.

acquisitions are given in Table 1. The analysis was done on a Sanders Model SA-240 Spectrum Analyzer. This instrument can ensemble average up to 512 spectra. A single spectrum is obtained in 25 ms.

The spectra of the hiss bands averaged for times that are much longer than the wave-particle interaction time are very smooth. When averaged for times comparable to the interaction time the spectra show considerable structure.

Several examples of spectra averaged for 6.4 s with a resolution of 5 Hz are shown in Fig. 7. Relative maxima are typically less than 2 db above adjacent minima.

Spectra with a resolution of 5 Hz obtained on a 200 ms sample of the broadband data show very large variations in amplitude between adjacent bins. Examples are shown in Figs. 8 and 9. Relative maxima here are often only one bin wide and 10 to 15 db above adjacent minima. Figure 8 shows two spectra obtained two seconds apart. Both are from the electric antenna. Figure 9 shows two spectra obtained 18 s apart. One is from the electric antenna the other is from the magnetic. There appears to be no correlation between the location of the relative maxima. This is a general characteristic of the spectra of the twenty cases analyzed.

Table 1. Parameters for the Chorus Events Studied

Date	Universal Time	Radial Distance, R_e	Local Time, hrs
6 Apr 79	04:30	6.2	11.8
7 May	19:30	5.3	15.1
12 May	14:20	6.7	10.1
23 Jun	00:15	5.4	11.3
29 Jun	19:50	5.8	8.4
3 Jul	16:10	6.1	6.5
10 Jul	00:00	6.6	18.6
17 Jul	06:30	5.4	12.2
19 Jul	17:50	5.9	15.4
26 Jul	10:30	5.4	8.1
3 Aug	12:20	6.1	14.5
6 Aug	08:30	5.4	10.9
19 Aug	04:30	5.6	12.0
30 Aug	03:45	6.8	15.9
4 Sep	03:00	7.1	16.4
11 Sep	08:35	7.4	22.0
11 Sep	23:00	6.9	15.2
21 Sep	17:25	6.3	12.9
22 Sep	14:30	5.6	9.8
29 Sep	15:50	6.9	14.0

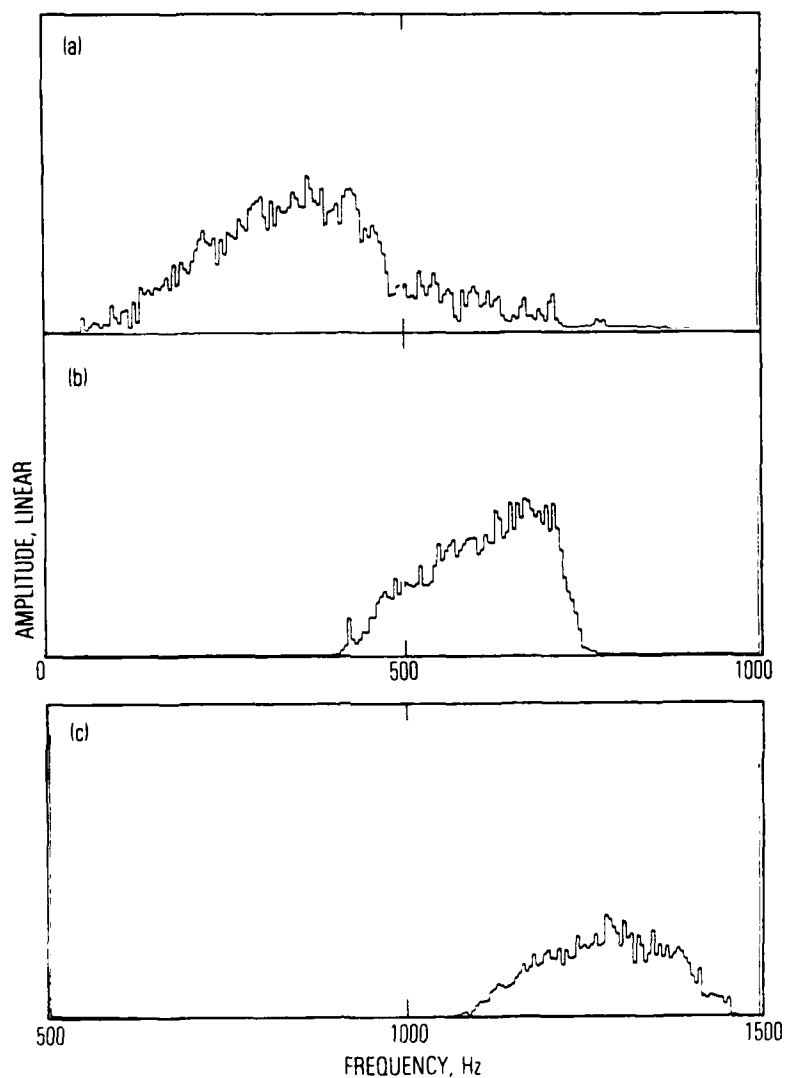


Figure 7. Hiss band spectra. Each spectrum is a 6.4 s linear ensemble average of 256 individual spectra. The individual spectra are obtained on contiguous 25 ms samples of the broadband data. The bin size is 5 Hz. The time periods correspond with the data in Fig. 1. (a) August 30, 1979, (b) July 9, 1979 and (c) July 19, 1979.

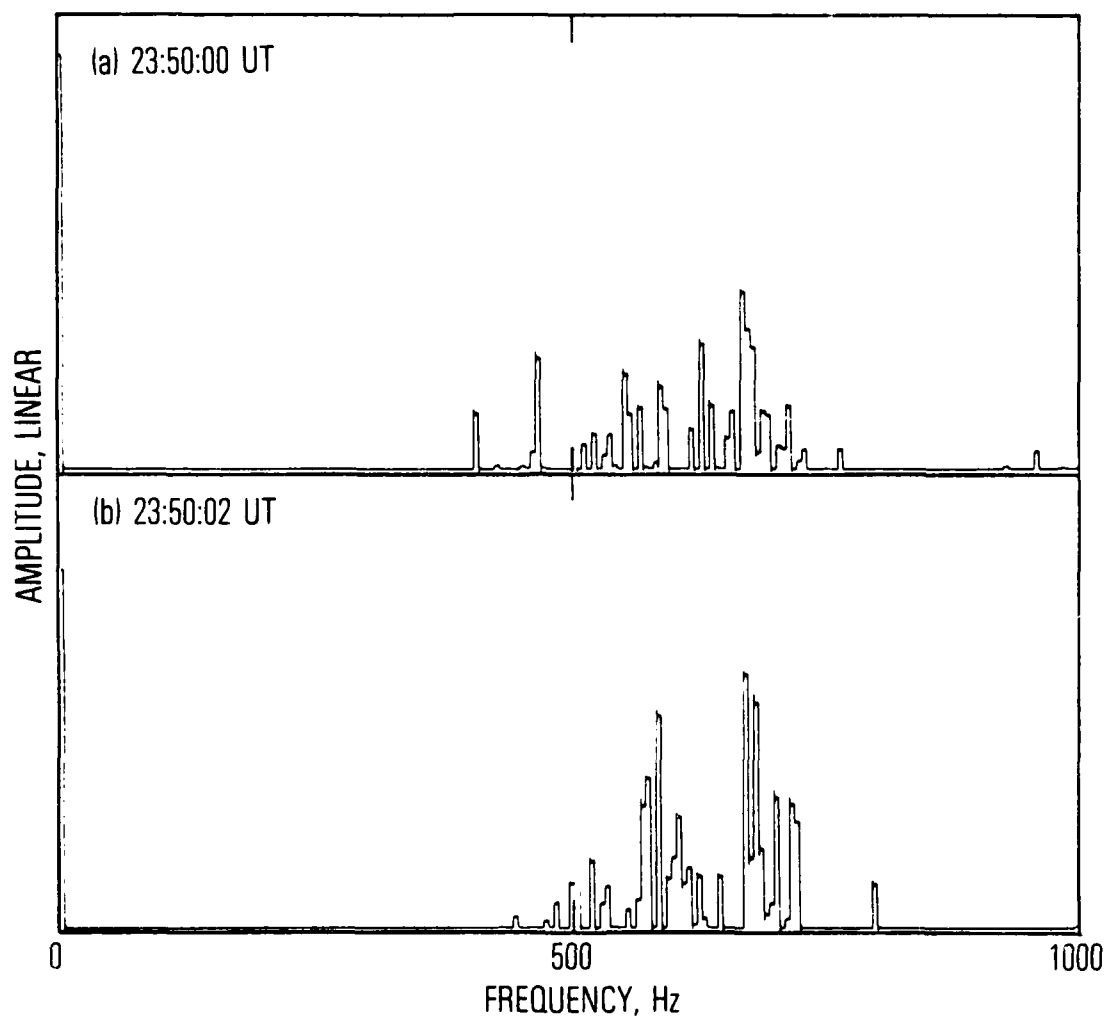


Figure 8. Hiss band spectra. Individual spectra obtained from 200-ms data samples from the electric antenna on July 9, 1979.

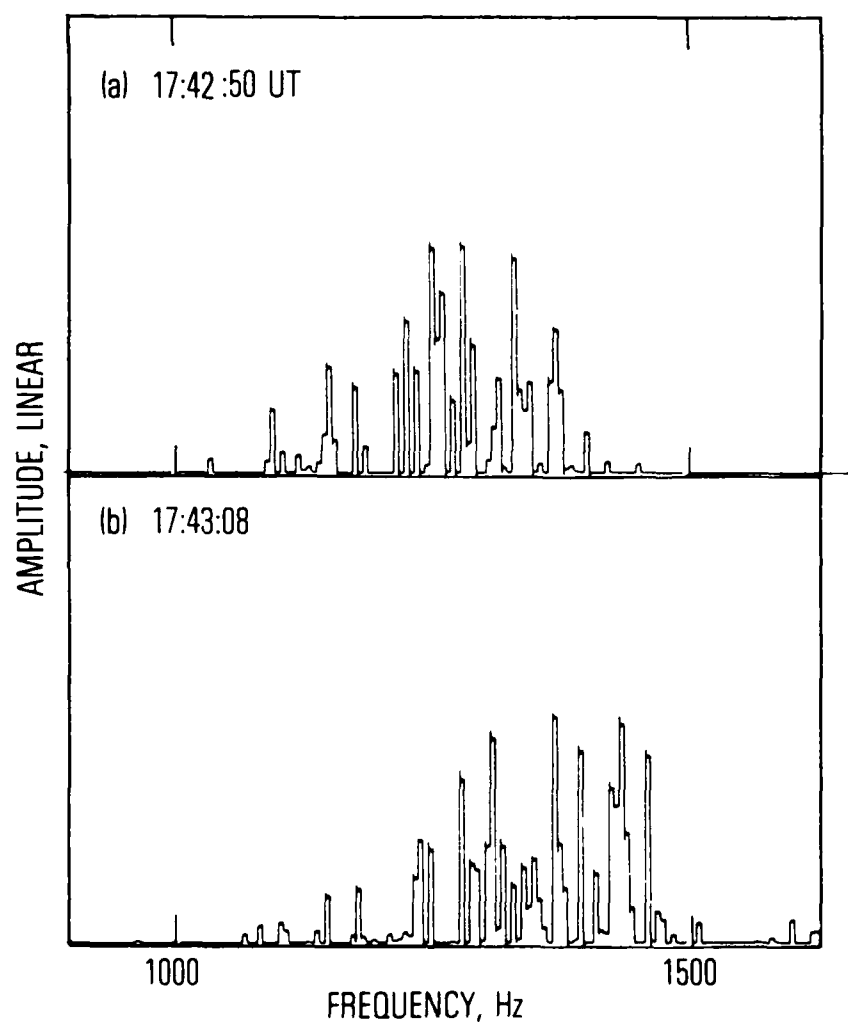


Figure 9. Hiss band spectra. Individual spectra obtained from 200-ms data samples from the electric antenna (a) and the magnetic antenna (b) on July 19, 1979.

IV. PARAMETRIC ANALYSIS

Electrons can be phase bunched while passing through a region occupied by a highly structured hiss band. Some of the electrons in a narrow energy range and pitch angle range see a large amplitude portion of the spectrum as a monochromatic wave if the bandwidth of the cyclotron resonance is comparable to or wider than the bandwidth of the maxima in the spectrum but not wide enough to include two maxima. These electrons will be phase bunched because they are not dephased by waves in adjacent parts of the spectrum.

As a model of this interaction mechanism we assume that electrons of a single energy and pitch angle are organized in phase by the doppler-shifted cyclotron resonance with waves of a single frequency, i.e., a local maximum in the hiss spectrum.

As the organized particles move away from the equator they generate an emission at the frequencies at which they resonate as they move adiabatically along the geomagnetic field line. The emitted waves propagate back toward the equator where they are detected by a receiver aboard the satellite. The shape of the emission is determined by the time delay as a function of frequency computed as the sum of the travel time of the electrons from the interaction region to the point of emission plus the propagation time of the waves to the point of detection. The cyclotron radiation portion of this model is essentially that proposed by Dowden [1962].

The motion of the locus of the radiation (interaction) region also modifies the spectral form of the emission [Helliwell, 1967]. Numerical calculations by Dowden [1962] show that the detail spectral shapes of emissions including 'hooks' and chorus can be accounted for by cyclotron radiation from

electrons spiraling along a magnetic field line. In this limiting case the locus of the interaction region moves with the initially phase-bunched electrons. More complicated spectral forms as discussed by Brice [1962] require the generalization proposed by Helliwell [1967].

The proposed chorus generation mechanism can be decomposed into two parts. The first is the phase bunching of the electrons in a hiss band. This takes place in an essentially stationary interaction region near the equator. The second is the coherent radiation by electrons in an interaction region that moves with the electrons along the field line.

In order to verify that phase bunching can occur we have computed the intrinsic bandwidth of the resonance, the wave-particle interaction time and the particle phase bunching time as a function of electron density at $L=6$. The phase bunching is assumed to take place at the magnetic equator. Relativistically correct equations are used and the pitch angle of the electrons at the equator is chosen to be 30 deg.

For equatorial cyclotron resonance the intrinsic bandwidth is $\Delta\omega/2\pi$, where $\Delta\omega$ is given [M. Schulz, 1972, 1974, 1975] by

$$\Delta\omega = |\pi^2 \bar{\omega}/2|^{1/3} [1 - (\mathbf{v}_\parallel/\hat{k} \cdot \bar{\mathbf{v}}_g) \cos \theta]^{-2/3} \quad (1)$$

where

$$\bar{\omega} = \frac{(3c/\omega_p L a)^2 (\Omega/\gamma - \omega)^3 [\omega(v+1 - \sec^2 \alpha) + \Omega (2/\gamma - v \cos \theta - \sec^2 \alpha \cos \theta)]}{2\omega \cos^2 \theta [1 - (\mathbf{v}_\parallel/\hat{k} \cdot \bar{\mathbf{v}}_g) \cos \theta]} \quad (2)$$

and

$$[1 - (v_{\parallel}/k \cdot \vec{v}_g) \cos \theta] = 1 + (\Omega/\gamma - \omega) \Omega \cos \theta / 2\pi (\Omega \cos \theta - \omega)$$

for the case of electron-cyclotron resonance for a relativistic electron with a whistler-mode wave with a wave-normal angle of θ with respect to \vec{B}_0 . The cold-plasma density is taken as proportional to B^v . The "gyrofrequency model" used in this paper corresponds to $v=1$. The factor in brackets on the right hand side of Eq. 1 is a correction to Eq. 4 of Schulz [1972].

To a stationary observer the length of a wave train that can interact with the particle is $\delta t [1 - (v_{\parallel}/k \cdot \vec{v}_g) \cos \theta]$ in time. The interaction time δt is related to the bandwidth $\Delta\omega/2\pi$ by

$$\Delta\omega/2\pi = (\delta t)^{-1} [1 - (v_{\parallel}/k \cdot \vec{v}_g) \cos \theta]^{-1} \quad (3)$$

Finally we must determine if there is sufficient time for the electrons to be phase bunched. Resonant electrons experience a longitudinal force and for small displacements from equilibrium in the potential well of the wave they oscillate at the trap oscillation frequency [Helliwell, 1967; Dowden et al. 1978]

$$\omega_t = \left(\frac{|e|}{m} B_w k v_{\perp} \right)^{1/2} \quad (4)$$

If the phases are initially random they become organized at times which are odd multiples of the phase bunching time

$$T_t = \frac{\pi}{2\omega_t} \quad (5)$$

The intrinsic bandwidth is plotted in Fig. 10 for three frequencies as a function of electron density at $L=6$. The energy of the corresponding resonant electrons with a pitch angle of 30 deg is shown in Fig. 11. Finally for this case the wave-particle interaction time and the phase-bunching time for a one picotesla wave intensity are shown in Fig. 12. Although one picotesla is a low amplitude for a hiss band it is representative of the wave intensities in a five Hertz bandwidth at the maxima in a structured hiss band. An example of broadband data showing one to two picotesla maxima calibrated using the 1.3 kHz narrowband channel data is shown in Fig. 13.

In Fig. 12 we note that at low density the interaction time is short compared with the phase-bunching time. We would expect chorus emissions to occur when the interaction time is comparable to or longer than the phase-bunching time. This occurs at the higher densities.

If the intrinsic bandwidth is too wide, more than one maximum may dephase the electrons. This would occur at low densities (Fig. 10). On the other hand if the intrinsic bandwidth is too narrow the peaks in the hiss band spectrum would not appear to the electrons as a monochromatic wave and phase bunching would not occur. This would occur at high densities (Fig. 10).

Etcheto et al. [1973] show that at a given L value the maximum power spectral density of ELF hiss is directly proportional to the cold plasma density. Since in our model hiss is a prerequisite for chorus we might expect chorus emissions to be more prevalent at higher densities. However the reduction in the intrinsic bandwidth as density increases will set an upper limit to the density at which chorus can be generated at a given L value. Combining all of these effects one would expect chorus to occur at $L=6$ when electron densities range from 3 to 30 cm^{-3} . Neither limit should be taken too literal-

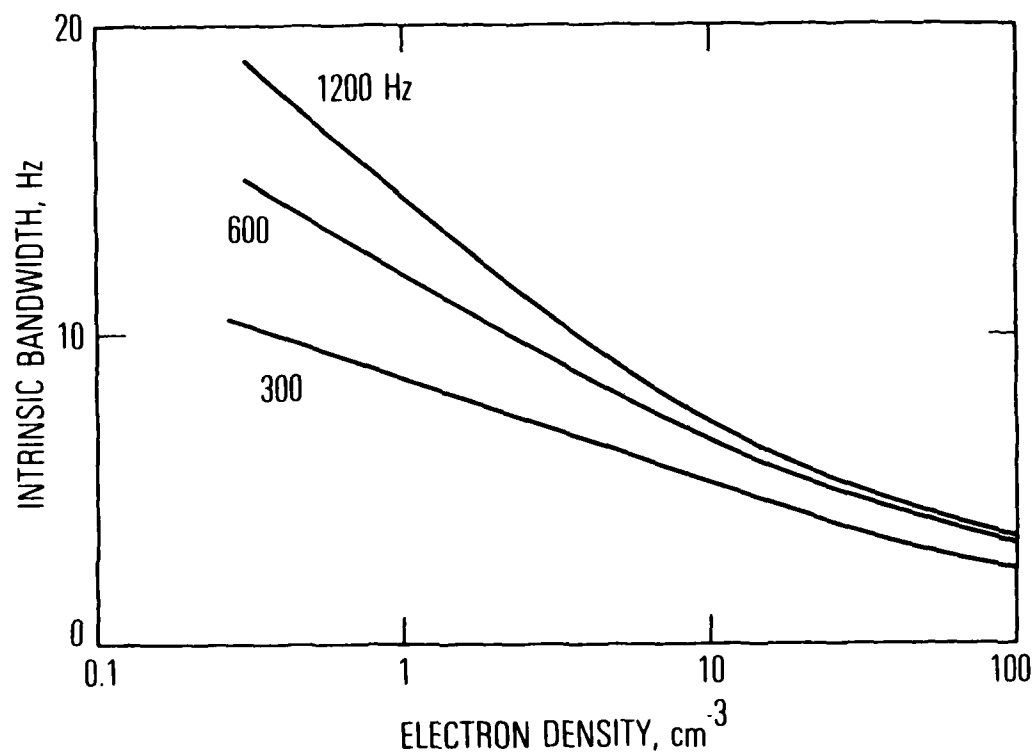


Figure 10. The intrinsic bandwidth of the doppler-shifted cyclotron resonance of energetic electrons with whistler-mode waves at the magnetic equator at $L=6$ as a function of the electron density. Curves are plotted for waves of three frequencies 300, 600 and 1200 Hz.

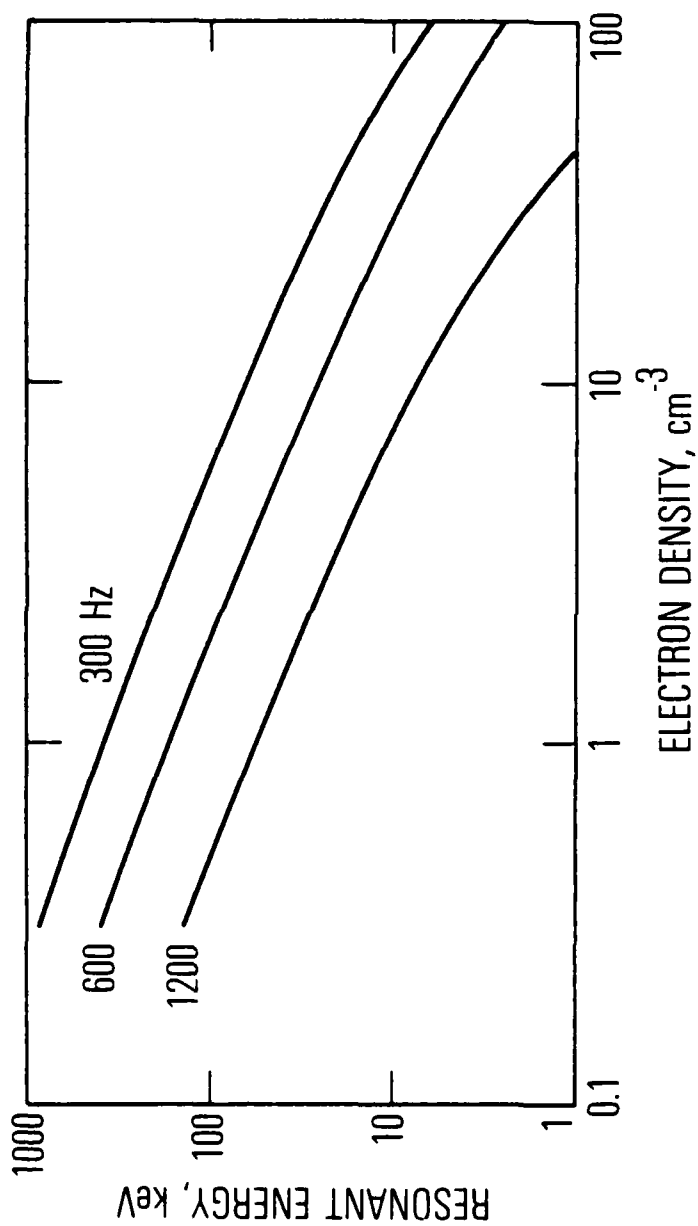


Figure 11. The energy of electrons with a pitch angle of 30 deg resonant with whistler-mode waves at the magnetic equator at $L=6$ as a function of the electron density. Curves are plotted for waves of three frequencies 300, 600 and 1200 Hz.

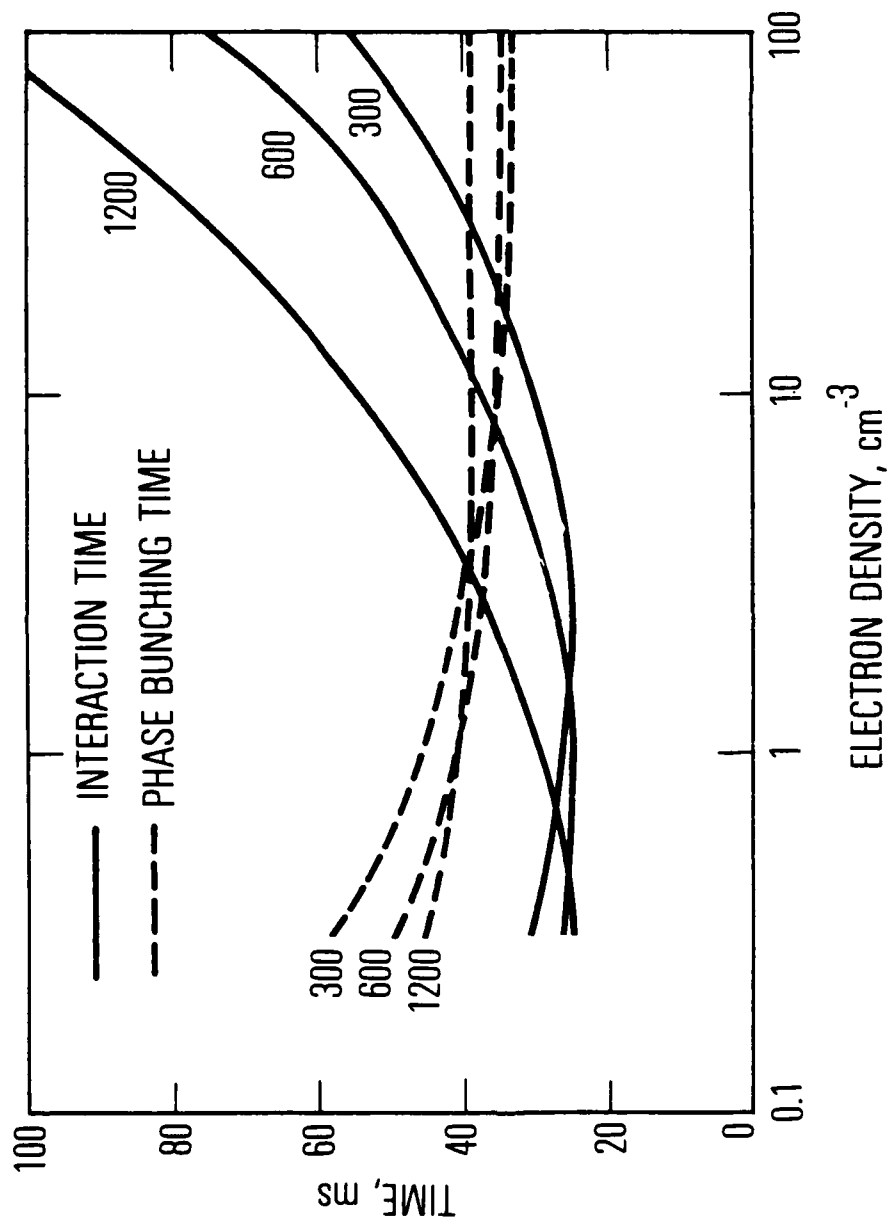


Figure 12. The wave-particle interaction time (solid curves) and the electron phase-bunching time (dashed curve) at the magnetic equator at $L=6$ as a function of the electron density. Curves are plotted for waves of three frequencies 300, 600 and 1200 Hz.

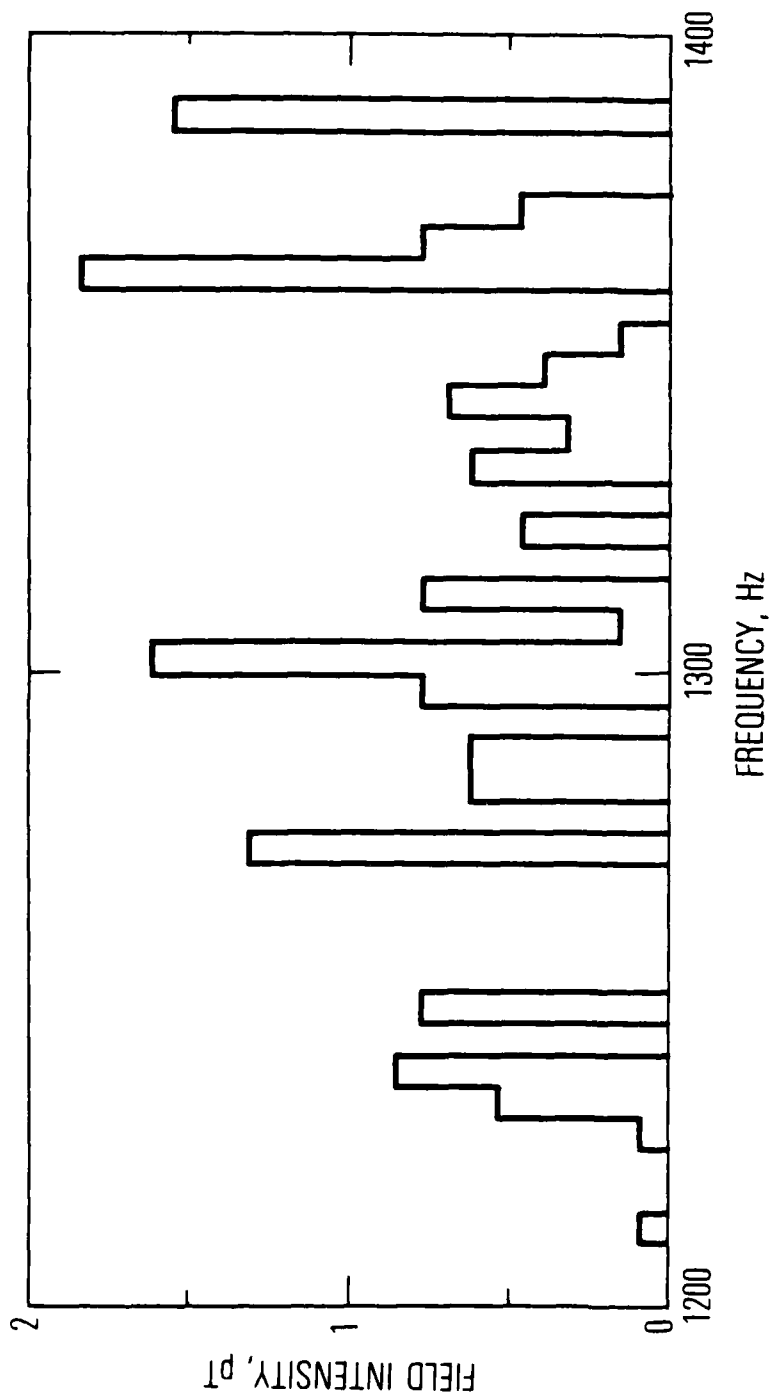


Figure 13. Individual hiss band spectrum obtained from a 200-ms data sample from the magnetic antenna on July 19, 1979. This is an expanded segment of the spectrum in Fig. 9b around 1300 Hz. It has been calibrated using the average amplitude of the 1300 Hz narrowband channel data at that time.

ly but this is the general range over which one would expect to observe chorus emissions.

V. NUMERICAL EXAMPLE

Detailed calculations based upon this emission mechanism have been carried out for a typical chorus emission detected by the SCATHA VLF receiver on April 6, 1979 (Fig. 2). A simplified model assuming wave propagation parallel to the geomagnetic field was used to obtain these numerical results. As the organized particles move away from the equator they generate an emission. The emitted waves propagate back toward the equator where they are detected by the SCATHA VLF receiver. The spectral shape of the emission is determined by the time delay as a function of frequency computed as the sum of the travel time of the electrons from the location of their phase bunching by the hiss to the point of emission plus the propagation time of the waves back to the point of detection.

A very general least squares fitting program was used to determine a spectral shape based upon this model to a set of frequency-time points (the circles in Fig. 14) taken from one of the chorus elements enlarged in Fig. 15. For this example the L-shell and latitude of the spacecraft were specified. A density model with electron density proportional to the magnetic field intensity was used and it was assumed that the electrons and waves traveled along the geomagnetic field line passing through the satellite. The fitting parameters were the interaction latitude, the equatorial electron density, the equatorial energy and pitch angle of the resonant electrons, and the starting frequency of the emission, i.e., the resonant frequency at the interaction latitude. The chorus emission is radiated by the electrons at the appropriate doppler-shifted cyclotron frequency as the electrons move adiabatically away from the equator. Since frequencies above one-half of the electron gyrofrequency, f_{bo} , will not propagate in a ducted mode and since it

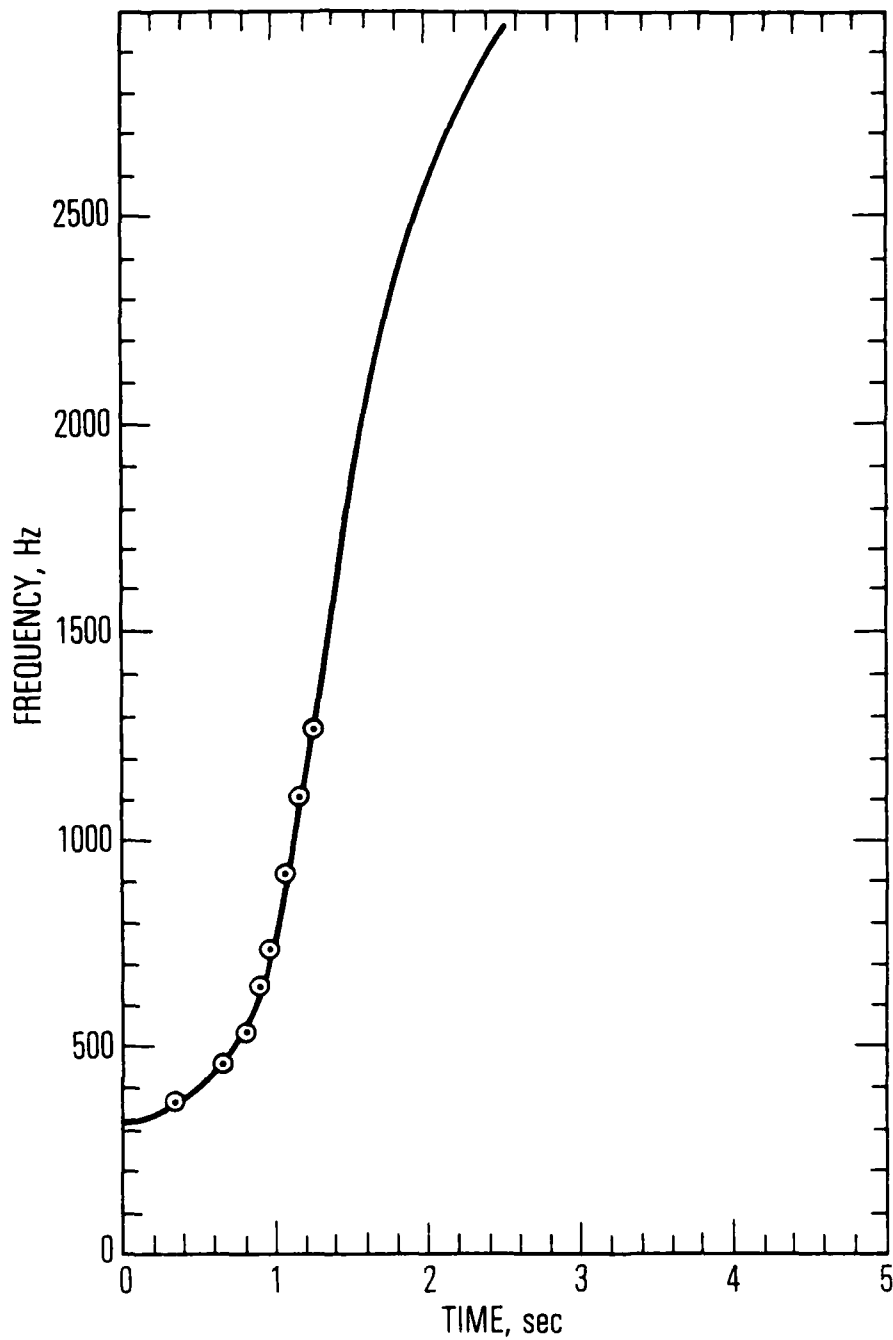


Figure 14. Parametric fit to a chorus element in Fig. 15. Parallel propagation was assumed. The circles are the data points input to the fitting routine.

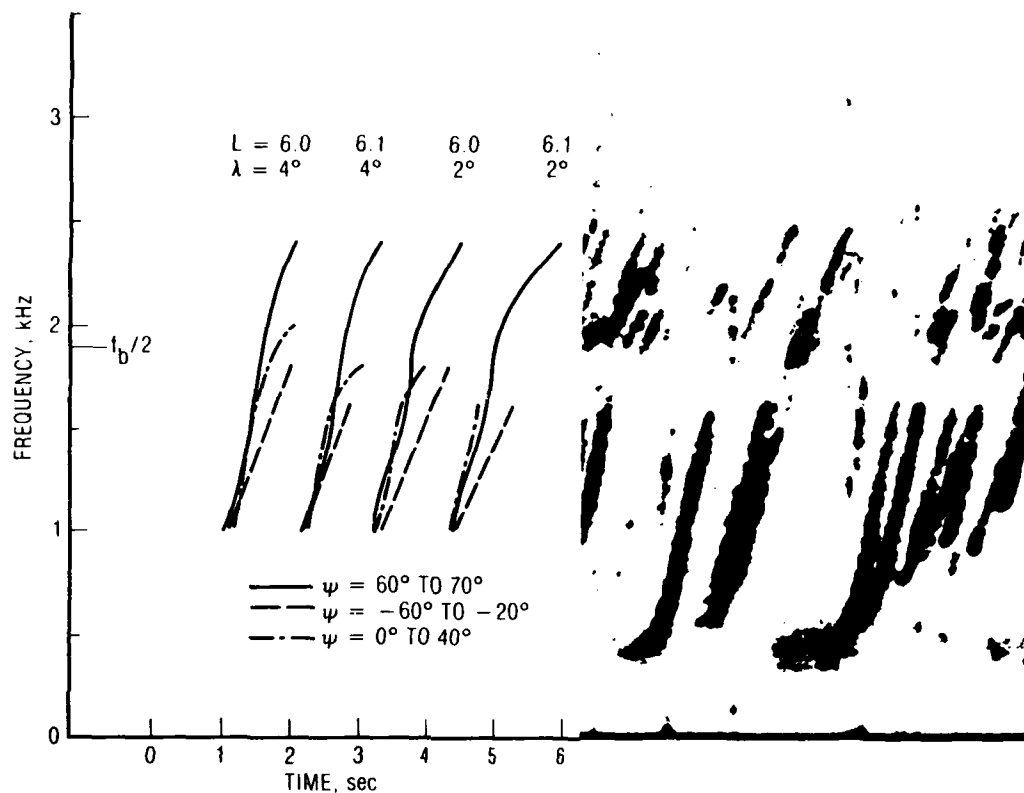


Figure 15. (left) Chorus elements computed using the parameters in Table 1 and a ray tracing program to obtain the time delays as a function of frequency for nonducted propagation to a detector located at the specified L-shell and magnetic latitudes, λ . Only frequencies above 1 kHz are shown. The shape below 1 kHz is essentially identical to that shown in Fig. 14. (right) Magnified chorus elements from Fig. 2 to compare with the computed spectral forms.

is improbable that this interaction is occurring in a duct, it is apparent that ray tracing from the emission point to the satellite is required to identify the propagation path and compute the correct shape of the chorus element.

Because it is impractical to use the least-squares fitting routine with the ray tracing program, the following compromise was chosen. At the lower frequencies the ray paths and travel times are not significantly different from those for propagation parallel to the field with zero wave normal angle. Only frequencies below $0.33 f_{bo}$ were used to obtain the fit and parallel propagation was assumed. The shape of the chorus element resulting from this calculation is shown in Fig. 14. The parameters giving the best fit are shown in Table 2. The result shows that 12.9 keV electrons with a pitch angle of 28 deg were phase-bunched 2.5 deg from the equator and subsequently radiated the chorus emission as they moved away from the equator. All of these values lie close to those used in the parametric study in the preceding section.

The only parameter that is somewhat suspect is the plasma density which seems high for an equatorial density at $L=6$. An independent calculation from the wave data confirms the value obtained. The index of refraction for the waves in the hiss band at 400 Hz can be computed from the data in Fig. 5 assuming that the wave normal angles are parallel to B_0 . The electric field, E_w , is 2.3×10^{-5} v/m. The magnetic field, B_w , is 3.5 pT. The index of refraction then is 45 and using the approximation $n^2 = \omega_p^2 / \omega \omega_b$ we obtain an electron density of 29 cm^{-3} . In the calculations that follow we shall use the value of 43 cm^{-3} obtained from the fit to the shape of the chorus element.

The parameters determined by the least-squares fitting technique described above were then used to compute the emission frequency vs. time profile at several points about the satellite location and over the entire frequency range of the observed chorus emissions. A two-dimensional ray tracing program was used to trace rays from the point of emission along the $L=6.06$ field line to the point of 'detection.' The emission frequency and wave normal angle are constrained to satisfy the doppler-shifted resonance condition for the electron parameters given in Table 2.

The chorus shapes are shown for four locations in Fig. 15. Typical ray paths to the actual location of the satellite at $L=6.06$ at a magnetic latitude of 3.6 deg are shown in Fig. 16.

Two important results come out of the ray tracing analysis. First, there are multiple paths to the 'detector' with slightly different time delays at the same frequency. This produces the emission triplets shown on the left hand side of Fig. 15. Second, large initial wave normal angles, ψ , are required to produce the frequencies above $f_b/2$ at the 'detector.' In our example the initial wave normal angles for these frequencies are between 60 and 70 deg with respect to the geomagnetic field direction. The shape of the emission is somewhat sensitive to the small changes in the 'detector' location used in this example.

For the parameter values given in Table 2 the intrinsic bandwidth $\Delta\omega/2\pi$, obtained from Eq. 1 is about 3 Hz. The interaction time δt obtained from Eq. 3 is 45 ms.

The interaction time is less than the length of the data sample (200 ms) used to compute the spectra shown in Figs. 8 and 9. The intrinsic bandwidth, 3 Hz, is comparable to the bin width, 5 Hz, in these spectra. Thus some domi-

Table 2. Chorus Element Model Parameters

Input Parameters:	
L-Shell	6.06
Geomagnetic field intensity	135 γ
Satellite latitude	-3.6 deg
Best Fit Model Parameters:	
Equatorial electron density	43 cm^{-3}
Interaction latitude	-2.35 deg
Interaction frequency	303 Hz
Resonant electron energy	12.9 keV
Equatorial pitch angle	28.3 deg

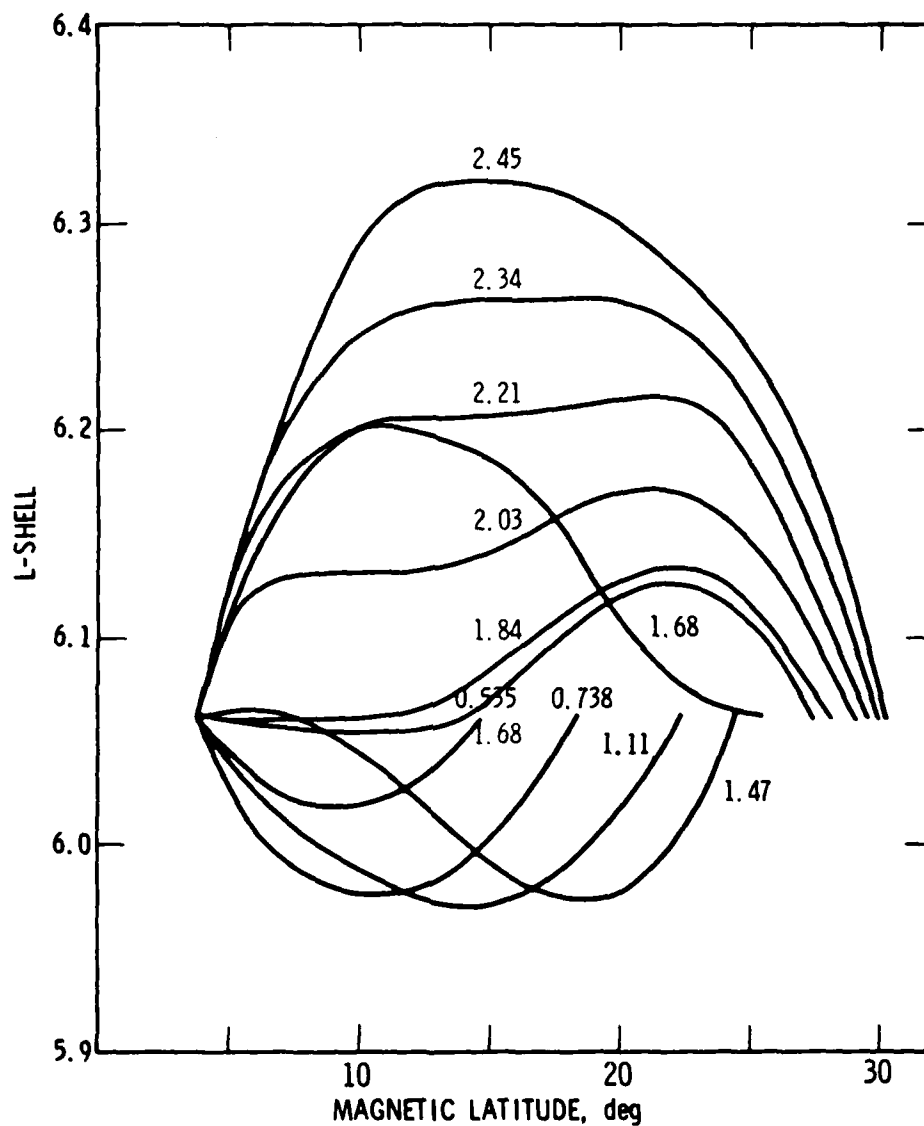


Figure 16. Typical nonducted chorus ray paths from the point of emission to the SCATHA satellite located on $L=6.06$ at a magnetic latitude of 3.36 deg. The curves are identified by the wave frequency in kilohertz.

nant local maxima should be seen by the resonant electrons as essentially monochromatic waves.

The phase bunching time for this example is 19 ms. Thus there is ample time for phase organization during a nominal interaction time of 45 ms.

This chorus triggering mechanism is essentially stochastic. A chorus emission occurs when the random wave spectrum produces sufficient phase organization for the nonlinear amplification of an embryo emission to take place.

Dowden et al. [1978] note that a weak input wave can have a significant effect on an interaction. The range of electron velocities trapped by an input wave is $v_0 \pm \frac{1}{2} \Delta v_{\parallel}$ where v_0 , the resonant velocity, and Δv_{\parallel} have values in this case appropriate to two adjacent local maxima, ω_1 and ω_2 , in the hiss band spectrum. The interaction range of the two waves will begin to overlap if

$$\begin{aligned} -\delta v_0 &= v_0(\omega_1) - v_0(\omega_2) \\ &= \frac{1}{2} \Delta v_{\parallel}(\omega_1) + \frac{1}{2} \Delta v_{\parallel}(\omega_2) \\ &= \beta \Delta v_{\parallel} \end{aligned}$$

where

$$\beta \equiv \frac{1}{2} [1 + \Delta v_{\parallel}(\omega_1)/\Delta v_{\parallel}(\omega_2)]$$

Dowden et al. [1978] derive a parameter

$$F_c = \frac{4 \omega \left[\left| \frac{e}{m} \right| B_w (\Omega - \omega) \right]^{1/2}}{\pi (\Omega + 2\omega) \beta}$$

When the frequency separation $|\omega_2 - \omega_1|/2\pi > F_c$, the coupling between the two waves is essentially zero. For the parameters given in Table 2, assuming equal amplitude waves, $F_c = 10$ Hz. Thus there would be no coupling between the interactions by adjacent maxima in the frequency spectrum of the hiss band. Although this is a non-relativistic calculation it is representative because the difference between the intrinsic bandwidths calculated using Eq. 3 and the nonrelativistic equivalent is only one percent.

VI. POWER LINE RADIATION

In the preceding section we have shown that chorus emission can be a natural stochastic process. Power line harmonic radiation thus is not necessary to trigger emissions. Radiation from power lines [Helliwell et al., 1975] and VLF ground based transmitters [Stiles and Helliwell, 1977] can trigger artificially stimulated emissions with characteristics that are essentially identical to chorus. Generally no hiss is present when this occurs. Thus PLR (at least propagating in a duct) is on occasion sufficient to generate chorus.

The important question to be answered is whether or not PLR plays a significant role in magnetospheric wave-particle interactions. Since most of the chorus events detected by SCATHA originate in hiss bands we must search for evidence for the PLR in the spectra of the hiss bands.

It is generally accepted that hiss is band-limited linear amplification of background noise [Etcheto et al., 1973]. In that case we must find evidence of amplified power line radiation in the hiss band or accept that it is not present at the level from which the ELF hiss is amplified. The sensitivity of the receiver is no longer in question because the hiss is typically a couple of orders of magnitude above the noise level of the receiver.

Typical spectra of hiss bands observed in the outer magnetosphere can be characterized as highly structured on short time scales (10's of milliseconds) but very smooth on long time scales (seconds). The spectrum on the longer time scales shows no evidence of monochromatic waves such as power line harmonic radiation. On the short time scale it would be difficult to establish the presence or absence of power line radiation. However the frequencies of

maxima in the spectra (see Figs. 8 and 9) are significantly closer together than the 100 to 120 Hz separation expected for the odd harmonics of power line radiation and the location of the peaks changes from one sample to the next producing the smooth spectrum on the average.

We find it impossible to accurately measure a monochromatic 'starting frequency' for chorus elements in the SCATHA data in the manner used by Lurette et al. [1979]. Virtually all of the elements appear to start with a small but finite slope and a subjective determination of their beginning varies with the gain of the analysis instrumentation and the photographic density of the image on the film. This should be a general characteristic of chorus detected by satellite receivers. It is improbable that the satellite would be located at the point where the electrons are initially phase bunched. Only here would the slope be zero at the start of an emission.

In order to determine if there is any statistical correlation between the frequency of the peaks in the spectra and power line harmonic frequencies we performed the following statistical analysis. Seven data acquisitions between 238 and 331 deg E. longitude were selected from the 20 acquisitions spectrum analyzed. These would be expected to have structure at harmonics of 60 Hz because the field lines passing through the satellite thread areas of the North American continent. Six spectra, three from the electric and three from the magnetic antenna, with a resolution of 5 Hz on a 200 ms data sample were used from each data acquisition. Time periods with well defined hiss and chorus emissions were chosen. The frequency range of the hiss band was determined from the ensemble average of 256 spectra. Fig. 17 shows a plot of the occurrence rate vs the difference in frequency between the largest amplitude peak within the hiss band and the nearest 60 Hz harmonic. Assuming that any frequency within the hiss band is equally likely a Chi-squared test of the

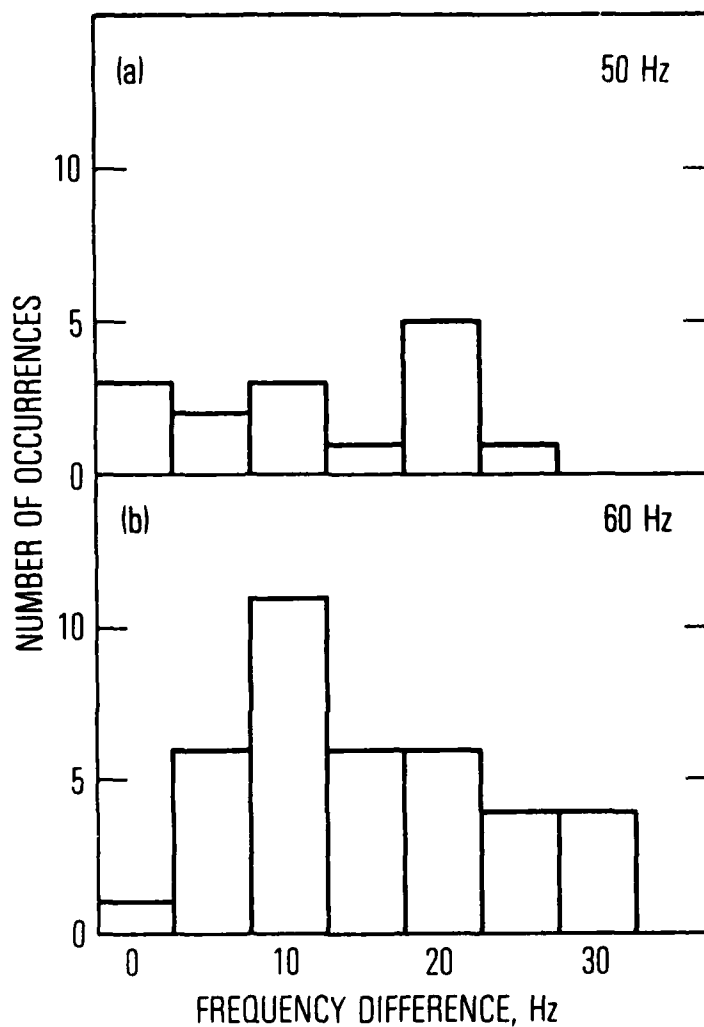


Figure 17. Measured frequency differences between dominant maxima in the hiss band spectra and the nearest power line harmonic. (a) Samples correlated with harmonics of 50 Hz from longitudes between 38 and 161 deg E. Long. (b) Samples correlated with harmonics of 60 Hz from longitudes between 239 and 331 deg E. Long.

data in Fig. 17 gives a probability of 0.42 that a random sample gives no better fit. We conclude that the distribution shows no evidence of 60 Hz harmonics in the hiss band spectra in agreement with their absence in the 6.4 s ensemble averages of the spectra. A similar result shown in Fig. 17 was obtained on a smaller sample looking for a correlation with 50 Hz harmonics in the eastern hemisphere. Data acquisitions in the Alaska - New Zealand sector were excluded from the samples.

A second and indirect argument that PLR is not generally present in the outer magnetosphere is the almost total absence of lightning generated whistlers in the broadband VLF data from SCATHA. In an atlas of emissions from the first year of operation only four acquisitions out of 890 show lightning generated whistlers. These four acquisitions were between 1300 and 1600 local time. Three were between $L = 5.4$ and 5.6 , near the satellite perigee, and one was at $L=6.3$. We conclude that whistler-mode signals from ELF sources including lightning and PLR in the earth-ionosphere waveguide are essentially absent in the outer magnetosphere.

VII. CONCLUSIONS

Chorus emissions can be generated by a natural stochastic process that occurs within highly structured hiss bands in the outer magnetosphere. In the model developed here the chorus element is doppler-shifted cyclotron radiation by electrons that have been phase bunched by waves in the hiss band. In the SCATHA data we find no evidence that monochromatic input waves such as power line harmonic radiation are present within the hiss bands from which chorus is being generated.

REFERENCES

- Brice, N. M., Discussion of paper by R. L. Dowden, 'Doppler-shifted cyclotron radiation from electrons: A theory of very-low-frequency emissions from the exosphere,' J. Geophys. Res., 67, 4897, 1962.
- Burtis, W. J., and R. A. Helliwell, Banded chorus - a new type of VLF radiation observed in the magnetosphere by OGO 1 and OGO 3, J. Geophys. Res. 74, 3002, 1969.
- Burtis, W. J. and R. A. Helliwell, Magnetospheric chorus: Occurrence patterns and normalized frequency, Planet. Space Sci., 24, 1007, 1976.
- Burton, R. K. and R. E. Holzer, The origin and propagation of chorus in the outer magnetosphere, J. Geophys. Res., 79, 1014, 1974.
- Cornilleau-Wehrlin, N., J. Etcheto and R. K. Burton, Detailed analysis of magnetospheric ELF chorus: Preliminary results, J. Atmos. Terr. Phys., 38, 1201, 1976.
- Cornilleau-Wehrlin, N., R. Gendrin, F. Lefeuvre, M. Parrot, R. Grard, D. Jones, A. Bahnsen, E. Ungstrup and W. Gibbons, VLF electromagnetic waves observed onboard GEOS-1, Space Sci. Rev., 22, 371, 1978.
- Coroniti, F. V., F. L. Scarf, C. F. Kennel, W. S. Kurth and D. A. Gurnett, Detection of Jovian whistler mode chorus; implications for the Io torus aurora, Geophys. Res. Lett., 7, 45, 1980.
- Dowden, R. L., Doppler-shifted cyclotron radiation from electrons: A theory of very low frequency emissions from the exosphere, J. Geophys. Res., 67, 1745, 1962.
- Dowden, R. L., Location of generation regions (in L and λ) of midlatitude VLF discrete emissions by dispersion analysis of ground station observations, J. Geophys. Res., 76, 1729, 1971.

- Dowden, R. L., A. D. McKay, L. E. S. Amon, H. C. Koons and M. H. Dazey, Linear and nonlinear amplification in the magnetosphere during a 6.6 kHz transmission, J. Geophys. Res., 83, 169, 1978.
- Etcheto, J., R. Gendrin, J. Solomon and R. Roux, A self-consistent theory of magnetospheric ELF hiss, J. Geophys. Res., 78, 8150, 1973.
- Helliwell, R. A., A theory of discrete VLF emissions from the magnetosphere, J. Geophys. Res., 72, 4773, 1967.
- Helliwell, R. A., J. P. Katsufakis, T. F. Bell and R. Raghuram, VLF line radiation in the earth's magnetosphere and its association with power system radiation, J. Geophys. Res., 80, 4249, 1975.
- Lurette, J. P., C. G. Park and R. A. Helliwell, Longitudinal variations of very-low-frequency chorus activity in the magnetosphere: Evidence of excitation by electrical power transmission lines, Geophys. Res. Lett., 4, 275, 1977.
- Lurette, J. P., C. G. Park and R. A. Helliwell, The control of the magnetosphere by power line radiation, J. Geophys. Res., 84, 2657, 1979.
- Schulz, M., Intrinsic bandwidth of cyclotron resonance in the geomagnetic field, Phys. Fluids, 15, 2448, 1972.
- Schulz, M., Wave-Particle Interactions in the Magnetospheric Plasma, Aerospace Corporation Technical Report ATR-74(7420)-1, The Aerospace Corporation, El Segundo, CA, 1974.
- Schulz, M., Resonance Broadening in a Turbulent Plasma, Aerospace Corporation Technical Report SAMSO-TR-75-185, The Aerospace Corporation, El Segundo, CA, 1975.
- Stiles, G. S. and R. A. Helliwell, Stimulated growth of coherent VLF waves in the magnetosphere, J. Geophys. Res., 82, 523, 1977.

Tsurutani, B. T., and E. J. Smith, Postmidnight chorus: A substorm phenomenon, J. Geophys. Res., 79, 118, 1974.

Tsurutani, B. T., and E. J. Smith, Two types of magnetospheric ELF chorus and their substorm dependences, J. Geophys. Res., 82, 5112, 1977.

Tsurutani, B. T., E. J. Smith, S. R. Church, R. M. Thorne and R. E. Holzer, "Does ELF chorus show evidence of power line stimulation?" in Wave Instabilities in Space Plasmas, eds. P. J. Palmadesso and K. Papadopoulos, D. Reidel Publ. Co., New York, 1979.

LABORATORY OPERATIONS

The Laboratory Operations of The Aerospace Corporation is conducting experimental and theoretical investigations necessary for the evaluation and application of scientific advances to new military concepts and systems. Versatility and flexibility have been developed to a high degree by the laboratory personnel in dealing with the many problems encountered in the Nation's rapidly developing space systems. Expertise in the latest scientific developments is vital to the accomplishment of tasks related to these problems. The laboratories that contribute to this research are:

Aerophysics Laboratory: Aerodynamics; fluid dynamics; plasmadynamics; chemical kinetics; engineering mechanics; flight dynamics; heat transfer; high-power gas lasers, continuous and pulsed, IR, visible, UV; laser physics; laser resonator optics; laser effects and countermeasures.

Chemistry and Physics Laboratory: Atmospheric reactions and optical backgrounds; radiative transfer and atmospheric transmission; thermal and state-specific reaction rates in rocket plumes; chemical thermodynamics and propulsion chemistry; laser isotope separation; chemistry and physics of particles; space environmental and contamination effects on spacecraft materials; lubrication; surface chemistry of insulators and conductors; cathode materials; sensor materials and sensor optics; applied laser spectroscopy; atomic frequency standards; pollution and toxic materials monitoring.

Electronics Research Laboratory: Electromagnetic theory and propagation phenomena; microwave and semiconductor devices and integrated circuits; quantum electronics, lasers, and electro-optics; communication sciences, applied electronics, superconducting and electronic device physics; millimeter-wave and far-infrared technology.

Materials Sciences Laboratory: Development of new materials; composite materials; graphite and ceramics; polymeric materials; weapons effects and hardened materials; materials for electronic devices; dimensionally stable materials; chemical and structural analyses; stress corrosion; fatigue of metals.

Space Sciences Laboratory: Atmospheric and ionospheric physics, radiation from the atmosphere, density and composition of the atmosphere, aurorae and airglow; magnetospheric physics, cosmic rays, generation and propagation of plasma waves in the magnetosphere; solar physics, x-ray astronomy; the effects of nuclear explosions, magnetic storms, and solar activity on the earth's atmosphere, ionosphere, and magnetosphere; the effects of optical, electromagnetic, and particulate radiations in space on space systems.

. . .

DATE
FILME